Science and Technology Indonesia
e-ISSN:2580-4391 *p*-ISSN:2580-4405
Vol. 7, No. 1, January 2022

Research Paper

Synthesis, Characterization, and Activity of The Photocatalyst Polyaniline (PANI)/TiO_2 in Degrading Rhodamine B Dye

Roy Andreas[1]*, Irmanto[1], Ades Oktaviani[1]

[1] *Department of Chemistry, Faculty of Mathematic and Natural Sciences, Jenderal Soedirman University, Banyumas, 53122, Indonesia*
***Corresponding Author e-mail: roy.andreas@unsoed.ac.id**

Abstract
The photocatalysts of Polyaniline (PANI) and composite Polyaniline /TiO_2 were syntheses by the interfacial polymerization (two-phase organic/water) method. The characteristics of the photocatalyst were identified by FTIR (Fourier Transform Infra-Red), SEM (Scanning Electron Microscopy), and EDX (Energy Dispersive X-ray Spectroscopy). The characteristic FT-IR peaks of Polyaniline and composite Polyaniline/TiO_2 are formed due to the formation H-Bonding. The XRD pattern shows that Polyaniline has a typical peak starting from 25.080 (2θ) planes (110) and amorphous polymer. The addition of TiO_2 (1%, 5% and 10% (w/w)) were found increased the activities. Photocatalyst Polyaniline/TiO_2 1% was proven to provide the highest reduction in Rhodamine B degradation, 53%. Rhodamine B degradation increased by 80% at pH 9 with an optimum time of 300 minutes under visible light from a tungsten lamp. The rate of kinetics was obtained following first order with a constant rate of photodegradation of 0.005445 minutes^{-1}.

Keywords
Polyaniline, Polyaniline/TiO_2, Rhodamine B, Photocatalyst

Received: 30 september 2021, Accepted: 23 January 2022
`https://doi.org/10.26554/sti.2022.7.1.126-131`

1. INTRODUCTION

The wastewater is mostly generated from textile industrial activities in Indonesia. Textile wastewater is a pollutant that contains hazardous substances. Rhodamine B, one of hazardous textile waste which is carcinogenic because it contains radical compounds that cause damage to the ecosystem. Photocatalytic is one method that can be used to overcome this problem. The inorganic semiconductor materials as photocatalysts to degrade wastewater have been widely studied (Afif et al., 2019; Di Paola et al., 2012; Radoičić et al., 2013; Salem et al., 2009; Sulaeman et al., 2016; Sulaeman et al., 2018). The best activity and high stability in photocatalytic reactions of organic or inorganic compounds are metal oxides composite (Andreas et al., 2019).

One type of organic material that can be used as a photocatalyst is Polyaniline (Gopalakrishnan et al., 2012). Polyaniline has advantages such as having a wide conductivity range, the synthesis process is easy and inexpensive, has high thermal stability, and has wide applications such as microelectronic materials, organic batteries, optics, sensors, transistors, batteries, capacitors, corrosive inhibitors, and photocatalysts (Haspulat et al., 2013; Andreas et al., 2019; Beek et al., 2005). Emeraldine base is one of the most stable forms of Polyaniline because its conductivity can be adjusted from 10-10 S/cm to 100 S/cm through protonic acid doping such as HCl (Nugroho et al., 2015).

Increasing the photocatalytic activity of Polyaniline is known to be done by making inorganic hybrid compounds, such as with TiO_2 including the formation of self-doping Polyaniline/-TiO_2 composites and their synergistic effect on the selective adsorption of heavy metals in wastewater (Chen et al., 2018), as well as the formation of Polyaniline/TiO_2 composites to degrade methylene blue dye (Yang et al., 2017). The photocatalytic activities of Polyaniline/TiO_2 were evaluated in the degradation of Methylene blue as model compounds and compared with the activity of bare colloidal TiO_2 nanoparticles (Radoičić et al., 2013).

This research was conducted to determine the increase in photocatalyst activity of Polyaniline with the addition of TiO_2 with various compositions (w/w), the synthesis was carried out using interfacial polymerization synthesis (Andreas et al., 2019). The effectiveness test of Polyaniline/TiO_2 photocatalyst will be carried out on Rhodamine B dye under the irradiation of a tungsten lamp.

2. EXPERIMENTAL SECTION

2.1 Materials and Instrumentation

Commercial aniline (99.5%), toluene, $(NH_4)_2S_2O_8$ (98%), HCl (35% GR), acetone and titanium dioxide (TiO_2) (from Merck) and distilled water. Composite characterization was carried out using UV-Vis spectrophotometer, FTIR, XRD, and SEM-EDX.

2.2 Synthesis of Polyaniline (PANI)

The synthesis of Polyaniline was carried out by the interfacial polymerization method. 50 mL toluene, 1 mL aniline mixed as organic phase and 50 mL of 1 M HCl, 0.6 g of $(NH_4)_2S_2O_8$ mixed as the aqueous phase. On the top is the toluene-aniline solution and the bottom is the solution of HCl-($(NH_4)_2S_2O_8$). The polymerization will start at the interface of the organic and the water phase and leave overnight. Polyaniline was purified by washing with HCl (0.2 M) and acetone, dried in an oven at 50°C for 5 hours.

2.3 Synthesis of Polyaniline/TiO_2

The Polyaniline/TiO_2 was prepared by comparing the TiO_2 weight ratio, using 0.040 g (1% w/w), 0.203 g (5% w/w), and 0.406 g (10% w/w) TiO_2 mixed with 4.060 g aniline and 200 mL toluene (in beaker glass). The mixture by a magnetic stirrer at a low temperature for 4 hours to form a suspension of the composite. Polymerization was carried out such as the synthesis of pure Polyaniline to obtain Polyaniline/TiO_2.

2.4 Characterization of Polyaniline and Polyaniline/TiO_2

The synthesized Polyaniline and Polyaniline/TiO_2 were characterized by XRD to determine the crystallite structure and sample purity, UV-Vis spectrophotometer to determine sample bandgap energy, FTIR to determine the absorption of organic functional groups present in the sample, and SEM-EDX to determine surface morphology, surface state and sample compositions.

2.5 Optimum Composition of PANI/TiO_2 in Degrading Rhodamine B

50 mL solution of Rhodamine B 20 ppm was prepared in a beaker. Each sample was added with 0.05 g of Polyaniline, TiO_2, 1%, 5%, and 10% Polyaniline/TiO_2. Each sample was stirred for 5 hours under a tungsten lamp. Samples were taken as much as 5 mL and then centrifuged. The Rhodamine B for all samples was analyzed by using a UV-Vis spectrophotometer at the maximum wavelength of Rhodamine B.

2.6 Optimum pH in Degrading Rhodamine B

Rhodamine B solution with a concentration of 20 ppm as much as 50 mL was added with a photocatalyst of Polyaniline or Polyaniline/TiO_2 which has the highest activity of 0.05 g. The samples were varied at pH 3, 5, 7, 9, and 11 using a solution of 0.5 M HCl and NaOH. The medium for the photocatalyst was stirred for 5 hours under a tungsten lamp and centrifuged. The Rhodamine B concentrations in all the samples were analyzed by using a UV-Vis spectrophotometer at the maximum wavelength of Rhodamine B.

2.7 Optimum Contact Time in Degrading Rhodamine B

Rhodamine B solution with a concentration of 20 ppm as much as 100 mL was added with a photocatalyst of Polyaniline or Polyaniline/TiO_2 which had the highest activity of 0.1 g and was conditioned at the optimum pH. Samples were varied depending on the length of contact time between the photocatalyst and Rhodamine B, which was within 8 hours. Samples were taken every 60 minutes. The concentration of Rhodamine B in the sample was analyzed by using a UV-Vis spectrophotometer at the maximum wavelength of Rhodamine B.

3. RESULT AND DISCUSSION

3.1 Characterization of Polyaniline/TiO_2

The results of the characterization using the PANI/TiO_2 composite SEM-EDX can be seen in Figure 1.

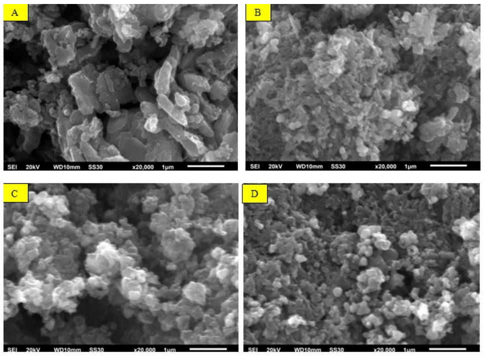

Figure 1. SEM Image A) Polyaniline , B) Polyaniline/TiO_2 1%, C) Polyaniline/TiO_2 5%, and D) Polyaniline/TiO_2 10% (w/w)

Figure 1 shows the morphology of the Polyaniline and Polyaniline/TiO_2 composites with different concentrations (1%; 5%; 10% w/w). The increasing percentage of TiO_2 caused the size of the particle to reduce. From the picture above, it can be seen that the size of TiO_2 crystals covered by Polyaniline decreases with increasing TiO_2. The agglomeration is caused by hydrogen bonding that occurs due to the interaction between TiO_2 and N-H (Eskizeybek et al., 2012; Mostafaei and Zolriasatein, 2012) or coordination bonds (Shukla et al., 2012). The SEM image concluded that the increasing of TiO_2 percentage influences the morphology of Polyaniline, since Polyaniline has various structures (granules, nanofiber, nanotubes, nanosphere, microspheres, and flake) (Stejskal et al., 2010).

Table 1 shows the Polyaniline or Polyaniline/TiO_2 dominated by carbon element from Polyaniline which is formed by the molecular formula $C_6H_5NH_2$. The result shows that the presence of oxygen and sulfur is thought to originate from ammonium peroxidisulphate ($(NH_4)_2S_2O_8$). Then the presence of chlorine is estimated to come from hydrochloric acid (HCl) as a material to produce protonated emeraldine.

The results of FTIR characterization can be seen in Figure 2. which shows that Polyaniline has a characteristic peak of about 2369.58 cm^{-1} (C-H stretch), C-N stretch of quinoid

Table 1. Average Weight (%) of Element Polyaniline dan Polyaniline/TiO_2

Element	Average Weight (%)			
	Polyaniline	Polyaniline/TiO_2 1%	Polyaniline/TiO_2 5%	Polyaniline/TiO_2 10%
C	72.42	78.96	73.83	66.65
N	16.35	16.01	15.55	14.15
O	1	16.35	17.27	19.39
S	0.50	0.37	0.38	0.77
Cl	3.26	2.48	3.87	5.74
Ti	0	1.16	3.75	6.20

units at wavenumbers 1224.79 cm^{-1}, 1220.11 cm^{-1}. N-H stretching occurred at 1683.50 and 1539.70 cm^{-1}. Polyaniline-/TiO_2 composites exhibited the same characteristic peaks as Polyaniline. However, peak displacement occurred when TiO_2 was added to Polyaniline. The peak shift occurred at wavenumbers 2362.90 cm^{-1}, 2385.69 cm^{-1}, and 2366.73 cm^{-1}. This is due to the hydrogen bonding between TiO_2 and the N-H groups on the Polyaniline chain (Eskizeybek et al., 2012).

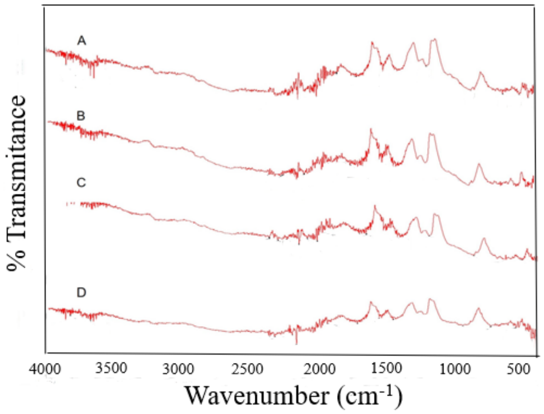

Figure 2. FTIR Spectra: A).Polyaniline, B).Polyaniline/TiO_2 1%, C).Polyaniline/TiO_2 5%, D).Polyaniline/TiO_2 10%

XRD analysis was then carried out to determine the formation of the PANI/TiO_2 composite which can be seen in Figure 3.

The XRD pattern shows that Polyaniline has a typical peak starting from 25.080 (2θ) planes (110), the characteristic peak of Polyaniline in the range 25-35 (2θ) cannot be observed because Polyaniline is an amorphous polymer, which is indicated by the presence of broad peaks and tends to be blunt. Furthermore, the 1%, 5%, 10% (w/w) Polyaniline/TiO_2 diffractograms also have more diverse peaks than the Polyaniline diffractograms. Pure titania only showed a photocatalytically active anatase phase at 2θ = 25.50 (101); 38 (004); 48.30 (200); 54 (105); 54 (105); 55.20 (211); 63 (204); and 68.90 (116) (JCPDS 21-1272).

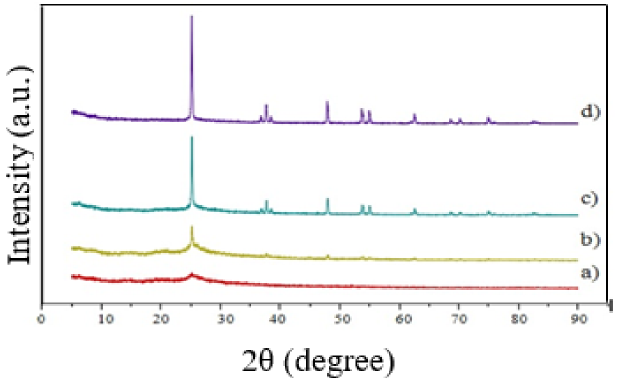

Figure 3. XRD Diffractogram from: a). Polyaniline, b). Polyaniline /TiO_2 1%, c). Polyaniline/TiO_2 5%, d). Polyaniline/TiO_2 10%

3.2 Optimum Composition in Degrading Rhodamine B

The activity test for the optimum Polyaniline/TiO_2 composition was carried out under the irradiation of a tungsten lamp as a light source.

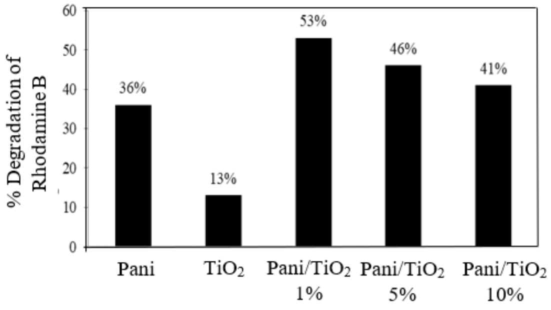

Figure 4. Diagram of Optimum Comparison of Polyaniline/TiO_2

Figure 4 shows the optimum composite composition is PANI/TiO_2 1% in degradation of Rodhamine B. The more TiO_2 is added (5% and 10%), it can increase the more agglomeration on the surface of the composite material. Increased agglomeration causes a smaller surface area so it has an impact on reducing photocatalytic activity. In addition, according to

Radoičić et al. (2013) the presence of structural defects can also occur in the Polyaniline chain due to the addition of excessive TiO_2. Structural defects cause changes in the electronic structure, increase polaron localization and reduce the conjugation system in the Polyaniline chain.

3.3 Optimum pH in Degrading Rhodamine B

The pH of the solution is one of the important parameters in the photodegradation process of Rhodamine B dyes because it will affect the surface charge of the photocatalyst, electrostatic interactions with Rhodamine B dye molecules, and determine the number of charged radicals generated during the photocatalytic process (Feng et al., 2014). By using the optimum composition of Polyaniline/TiO_2 (1% w/w), the effect of the pH on the percentage of degradation Rhodamine B is shown in Figure 5.

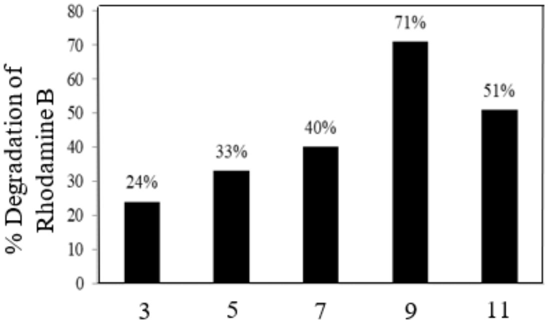

Figure 5. Effect of pH on Rhodamine B Degradation

The addition of acid can increase the H^+ species in the solution which can reduce the contact between the photocatalyst and Rhodamine B and in the acidic pH state, Rhodamine B is cationic, therefore electrostatic repulsion can occur between Rhodamine B and TiO_2 photocatalyst which can reduce photodegradation efficiency. It is known that Polyaniline/TiO_2 photocatalyst has the highest activity at pH 9. At alkaline pH, Rhodamine B will be deprotonated to form a zwitterion structure, the following is the structure of Rhodamine B at acidic and basic pH.

The structure of Rhodamine B which forms zwitterions at alkaline pH causes the formation of bonds between the photocatalyst and Rhodamine B. At alkaline pH, TiO_2 will be negatively charged and bind to the positively charged N-ethylenediamine site. Meanwhile, Polyaniline will attack the negatively charged carboxyl group. Polyaniline is a selective adsorbent for anionic dyes because it has a positive charge and Polyaniline will electrostatically attract negatively charged anionic dyes (Jumat et al., 2017). This causes the photocatalytic activity to increase at alkaline pH, according to that a higher pH indicates an abundance of OH^-, and results in increased •OH formation (Yang et al., 2017).

3.4 Optimum Contact Time in Degrading Rhodamine B

The optimum contact time (Polyaniline/TiO_2 1% and pH 9) can be seen in Figure 6, the optimum time is obtained at 300 minutes and then constant until 400 minutes.

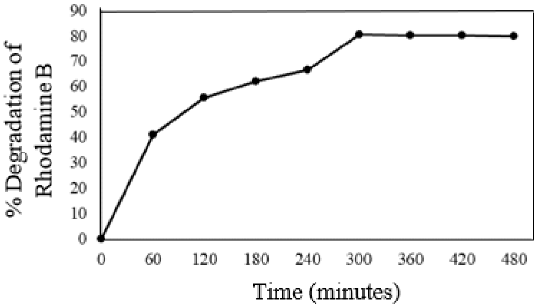

Figure 6. Effect of Time on Rhodamine B Degradation

The results showed that the increased contact time caused an increase in the percent degradation of Rhodamine B. This is because the longer the contact time between the photon and the photocatalyst, the more superoxide (•O_2) and hydroxyl radicals (•OH) are formed which function as oxidizing agents in the degradation process of Rhodamine B. The photocatalytic process occurs when the photocatalyst is exposed to irradiation of a tungsten lamp which has an energy that matches or even exceeds the bandgap energy of the photocatalyst, the electrons in the valence band of the photocatalyst will be excited to the conduction band which will produce electrons (e^-) and vacancies or holes (h^+) which act like positive charges that play a role in degrading dyestuffs, it is known that in this photocatalytic process OH is the dominant species that play a role in degrading dyestuffs, namely the destruction of the chromophore group of Rhodamine B produces simpler intermediates and the final products are CO_2 and H_2O (Riyani et al., 2021).

3.5 Photocatalytic Kinetics Rate and Mechanism in Degrading Rhodamine B

Determination of the zero-order is done by graphing the concentration of Rhodamine B at time t versus time. The determination of the first order is done by making a graph between the concentration of Rhodamine B (at the time) t divided by the initial concentration (C_0) against time. Determination of the order of the second reaction is carried out by plotting 1/Ct against time when comparing the value of R^2 from the linear regression equation obtained from each reaction order.

In determining the kinetics of the photocatalytic rate, it was obtained that it was of the first order. Figure 8 shows the plot of ln C_0/C against photodegradation time of Rhodamine B by 1% Polyaniline/TiO_2 composites.

The plot of ln C_0/C vs time was used to determine the rate constant (k) of photodegradation. If we use the first-order kinetic rate equation, the photodegradation rate constant can be calculated using the following equation.

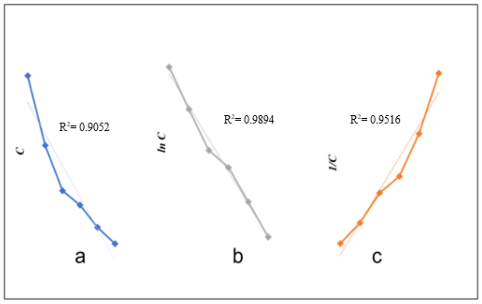

Figure 7. Reaction Rate Curves a) Zero-Order, b) First Order and c) Second-Order

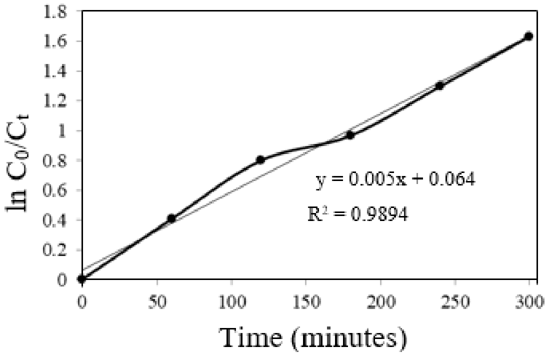

Figure 8. ln C_0/C vs Time of Rhodamine B Degradation

$$\ln C = -k.t + \ln C_0 \tag{1}$$

$$k.t = \ln \frac{C_0}{C} \tag{2}$$

$$k = \frac{\ln \frac{C_0}{C}}{t} \tag{3}$$

The results showed that the rate of photodegradation of Polyaniline/TiO_2 in degrading Rhodamine B was 0.005445 min^{-1}.

According to Yang et al. (2017), with the results of UV-DRS analysis, the mechanism of Polyaniline/TiO_2 photocatalyst is obtained as follows:

The material-doped Polyaniline semiconductor absorb visible light irradiation and transfer photogenerated electrons (e^-) to the Conduction Band (CB) of TiO_2. Simultaneously, the h^+ generated in the Valence Band (VB) of TiO_2 is transferred to HOMO on Polyaniline. This electron transfer between Polyaniline and the TiO_2 semiconductor results in free electrons (e^-) reacting with O_2 to produce superoxide radicals ($\bullet O_2$), and holes (h^+) reacting with OH and H_2O to produce hydroxyl radicals (•OH). Then the target compound will be degraded by Reactive Oxygen Species (ROS) ($\bullet O_2$ and •OH). The reaction of the photocatalytic mechanism of Polyaniline/TiO_2 is as follows:

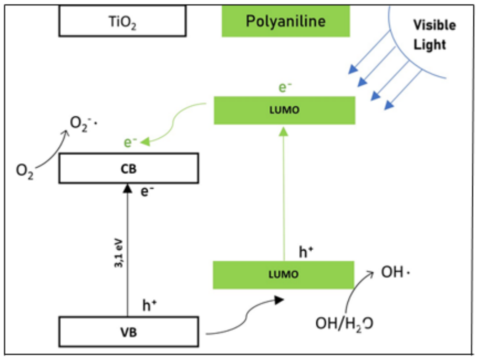

Figure 9. Mechanism of Polyaniline/TiO_2 Photocatalysis

Polyaniline/TiO_2 + hv → Polyaniline/TiO_2 + e^-
$e^- + O_2 \rightarrow \bullet O_{2-}$
Polyaniline$^+$/TiO_2 → Polyaniline$^+$/TiO_2 + h^+
$h^+ + H_2O/OH^- \rightarrow \bullet OH$
RhB + ROS → intermediet product → CO_2 + H_2O

4. CONCLUSION

Based on the research conducted, it was found that the synthesized Polyaniline/TiO_2 composite was in the form of emeraldine salt in the form of a dark green precipitate. The photocatalytic activity test showed that the Polyaniline/TiO_2 photocatalyst could reduce the concentration of Rhodamine B by 80% at pH 9 for 300 minutes with a photodegradation rate of 0.005445 $minutes^{-1}$.

5. ACKNOWLEDGEMENT

This research was financially supported by DIKTI, Ministry of Research, Technology and Higher Education of Republic of Indonesian the Scheme of *Program Penelitian Dasar*.

REFERENCES

Afif, M., U. Sulaeman, A. Riapanitra, R. Andreas, and S. Yin (2019). Use of Mn Doping to Suppress Defect Sites in Ag_3PO_4: Applications in Photocatalysis. *Applied Surface Science*, **466**; 352–357

Andreas, R., A. Lesbani, and F. A. Yusuf (2019). The Character Istics (Compositions, Morphological, and Structure) of Nanocomposites Polyaniline (PANI)/ZnO. *IOP Conference Series: Materials Science and Engineering*, **509**; 012126

Beek, W. J., L. H. Slooff, M. M. Wienk, J. M. Kroon, and R. Janssen (2005). Hybrid solar cells using a zinc oxide precursor and a conjugated polymer. *Advanced Functional Materials*, **15**(10); 1703–1707

Chen, J., N. Wang, Y. Liu, J. Zhu, J. Feng, and W. Yan (2018). Synergetic Effect in a Self-Doping Polyaniline/TiO_2 Composite for Selective Adsorption of Heavy Metal Ions. *Synthetic Metals*, **245**; 32–41

Di Paola, A., E. García-López, G. Marcì, and L. Palmisano (2012). A Survey of Photocatalytic Materials for Environmental Remediation. *Journal of Hazardous materials*, **211**; 3–29

Eskizeybek, V., F. Sarı, H. Gülce, A. Gülce, and A. Avcı (2012). Preparation of The New Polyaniline/ZnO Nanocomposite and its Photocatalytic Activity for Degradation of Methylene Blue and Malachite Green Dyes Under UV and Natural Sun Lights Irradiations. *Applied Catalysis B: Environmental*, **119**; 197–206

Feng, X., H. Guo, K. Patel, H. Zhou, and X. Lou (2014). High performance, Recoverable Fe_3O_4ZnO Nanoparticles for Enhanced Photocatalytic Degradation of Phenol. *Chemical Engineering Journal*, **244**; 327–334

Gopalakrishnan, K., M. Elango, and M. Thamilselvan (2012). Optical studies on nano-structured conducting Polyaniline prepared by chemical oxidation method. *Archives of Physics Research*, **3**(4); 315–319

Haspulat, B., A. Gülce, and H. Gülce (2013). Efficient Photocatalytic Decolorization of Some Textile Dyes Using Fe Ions Doped Polyaniline Film on ITO Coated Glass Substrate. *Journal of Hazardous Materials*, **260**; 518–526

Jumat, N. A., P. S. Wai, J. J. Ching, and W. J. Basirun (2017). Synthesis of Polyaniline-TiO_2 Nanocomposites and their Application in Photocatalytic Degradation. *Polymers and Polymer Composites*, **25**(7); 507–514

Mostafaei, A. and A. Zolriasatein (2012). Synthesis and Characterization of Conducting Polyaniline Nanocomposites Containing ZnO Nanorods. *Progress in Natural Science: Materials International*, **22**(4); 273–280

Nugroho, M. W., A. Riapanitra, and P. Iswanto (2015). Sintesis Nanokomposit Polianilin/ZnO Dengan Metode PolimerisasiI Antarmuka dan Uji Aktivitas Fotodegradasinya Terhadap Rhodamin B Pada Cahaya Tampak. *Molekul*, **10**(2); 121–128. (in Indonesia)

Radoičić, M., Z. Šaponjić, I. A. Janković, G. Ćirić-Marjanović, S. P. Ahrenkiel, and M. Čomor (2013). Improvements to The photocatalytic Efficiency of Polyaniline Modified TiO_2 Nanoparticles. *Applied Catalysis B: Environmental*, **136**; 133–139

Riyani, K., T. Setyaningtyas, and A. Riapanitra (2021). Degradation of Phenol in Batik Industry Wastewater Using thin Layer TiO_2 Photocatalyst. *IOP Conference Series: Earth and Environmental Science*, **746**; 012031

Salem, M. A., A. F. Al-Ghonemiy, and A. B. Zaki (2009). Photocatalytic Degradation of Allura Red and Quinoline Yellow with Polyaniline/TiO_2 Nanocomposite. *Applied Catalysis B: Environmental*, **91**(1-2); 59–66

Shukla, S., M. Vamakshi, A. Bharadavaja, A. Shekhar, and A. Tiwari (2012). Fabrication of Electro-Chemical Humidity Sensor Based on Zinc Oxide/Polyaniline Nanocomposites. *Advance Material Letters*, **3**(5); 421–425

Stejskal, J., I. Sapurina, and M. Trchová (2010). Polyaniline Nanostructures and The Role of Aniline Oligomers in their Formation. *Progress in Polymer Science*, **35**(12); 1420–1481

Sulaeman, U., F. Febiyanto, S. Yin, and T. Sato (2016). The Highly Active Saddle-Like Ag_3PO_4 Photocatalyst Under Visible Light Irradiation. *Catalysis Communications*, **85**; 22–25

Sulaeman, U., D. Hermawan, R. Andreas, A. Z. Abdullah, and S. Yin (2018). Native Defects in Silver Orthophosphate and their Effects on Photocatalytic Activity Under Visible Light Irradiation. *Applied Surface Science*, **428**; 1029–1035

Yang, C., W. Dong, G. Cui, Y. Zhao, X. Shi, X. Xia, B. Tang, and W. Wang (2017). Enhanced photocatalytic Activity of PANI/TiO_2 Due to their Photosensitization-Synergetic Effect. *Electrochimica Acta*, **247**; 486–495